BUTTERWORTH HEINEMANN

J. Proc. Cont. Vol. 5, No. 4, pp. 249–261, 1995

0959-1524/95 $10.00 + 0.00

0959-1524(95)00017-8

Opportunities and difficulties with 5 × 5 distillation control

Petter Lundström* and Sigurd Skogestad†

Chemical Engineering Department, University of Trondheim (NTH), N-7034 Trondheim, Norway

Multivariable 5 × 5 distillation control, i.e., control of levels, pressure and compositions by one multivariable controller, provides opportunities to improve the control performance as compared to decentralized control. Multivariable interactions can be counteracted with a 5 × 5 controller. However, the main advantage is automatic constraint handling which cannot be realized by a fixed linear 5 × 5 controller, but requires a solution based on on-line optimization, for example, using a model predictive control (MPC) strategy. A multivariable control scheme also presents some difficulties. Unconsidered model uncertainty may be a severe problem. It may also be difficult to tune the multivariable controller. In this paper the MPC approach is combined with the $\mathcal{H}_\infty/\mu$ framework in order to obtain a robust design.

A one-feed two-product distillation column as shown in *Figure 1*, may be viewed as a 5 × 5 dynamic system. This means that for a fixed design and a given feed the column has five (dynamic) degrees of freedom, or in control terms, there are five manipulated inputs which may be used to control five controlled outputs.

The five controlled variables (outputs) are the liquid holdup in reboiler and condenser (M_B, M_D, here assumed on a molar basis), pressure in the condenser (P_D), composition of light component in the top product (distillate) (x_D) and composition of light component in the bottom product (bottoms) (x_B). In this paper all controlled outputs are measured, but measurement errors are included in the analysis. The five manipulated variables (inputs) are the flows of reflux, distillate and bottoms (L_T, D and B, here assumed on a molar basis), and the heat duty in reboiler and condenser (Q_R, Q_C). The feed rate (F), composition (z_F) and energy content (defined in terms of the bubble point pressure of a liquid feed, P_F^{sat}) all act as disturbances. In addition, there are disturbances in all the manipulated variables.

In industry most columns are operated by single-input-single-output (SISO) controllers and manual adjustments. Such a decentralized (multiloop) control structure has the advantage of being easy to retune and to understand. However, fixed pairing of outputs and inputs may limit the performance of the overall system, since the SISO controllers do not utilize information from the other loops. Another disadvantage with decentralized control is that the control performance may seriously deteriorate if the system hits some constraint. For example, if a stabilizing loop saturates, the system goes unstable. To avoid this, the plant has to be operated sufficiently far away from the constraints, or facilities for loop reconfiguration have to be installed 'on-top' of the SISO controllers.

From a theoretical point of view it is obvious that the 'optimal' controller should use all available information (measurements, plant model, expected model uncertainty, expected disturbances, known future setpoint changes, known constraints, etc.) to manipulate all five

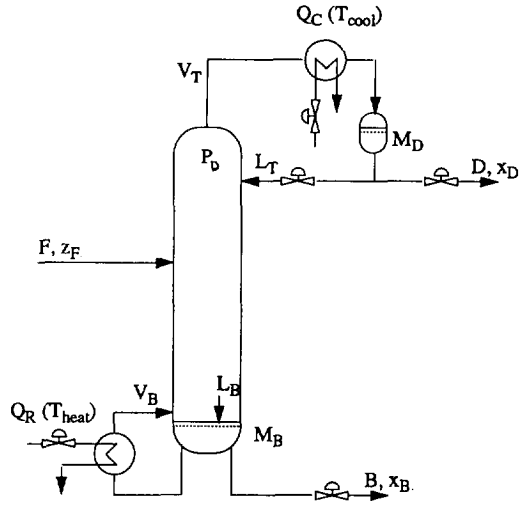

Figure 1 One-feed two-product distillation column

*Present address: Norcontrol Systems a.s., PO Box 1024, N-3194 Horten, Norway.
†Author to whom correspondence should be addressed. E-mail: skoge@kjemi.unit.no

inputs in order to keep all five outputs at their optimal values (5 × 5 control)[1]. It is also clear that constraint handling is a very important issue for this 'optimal' control scheme, since, in general, optimality is obtained at some constraint, for example, maximum throughput.

A fundamental difficulty with any optimizing scheme is to define an objective function which yields a mathematically optimal solution in agreement with what is actually desired. Another problem is to obtain sufficiently accurate information (measurements, plant model, uncertainty bounds etc.) to make the optimization worthwhile.

The purpose of this paper is to evaluate the opportunities and difficulties with applying 5 × 5 control to a distillation column. The paper is organized as follows. In the next section we present a fairly rigorous non-linear 5 × 5 model, which, contrary to most other distillation models, does not assume constant pressure (which would yield a 4 × 4 model). In the following section we perform a controllability study using a linearized model. We also consider a decentralized controller which leads to a rather poor performance for the example column in question. We then study the unconstrained multivariable problem, using the $\mathcal{H}_\infty$-norm to measure control performance. This norm makes it possible to specify desired responses in terms of closed-loop time constants, allowable steady stage offset and acceptable overshoot, and also allows us to address robustness using the structured singular value[2], μ. We then consider model predictive control using a state observer based MPC algorithm[3]. To obtain a robust controller, we first attempt to tune the unconstrained MPC controller to mimic the performance of the robust $\mathcal{H}_\infty/\mu$ controller by using μ-analysis and the weights obtained from the $\mathcal{H}_\infty$ design. Of course, this may not be done directly, as an MPC controller behaves similarly to an $\mathcal{H}_2$-controller, which is not quite the same as an $\mathcal{H}_\infty$-controller (the norms are somewhat different). When the unconstrained performance has been assessed using μ, we use simulations to evaluate the performance for the constrained case.

5 × 5 distillation model

In this section we briefly present the distillation column which is used as an example process in the rest of the paper. The example column separates a binary mixture into a top and a bottom product of relatively high purity (99%). The column closely matches 'column A' studied by Skogestad and Morari[4], but the model used here is much more detailed:

1. Pressure is not assumed constant.
2. Vapour holdup is included.
3. Vapour flow rate from one tray to another is computed from the pressure difference between the trays.
4. Liquid flow rate is computed from the Francis weir formula, including a correlation between vapour flow and froth density[5] such that a change in vapour flow will have an initial effect on the liquid flow (the 'K_2'-effect)[6].
5. Energy balance is included, but we have assumed that the two components have the same values for the heat of vaporization, c_{PL} and c_{PV}.

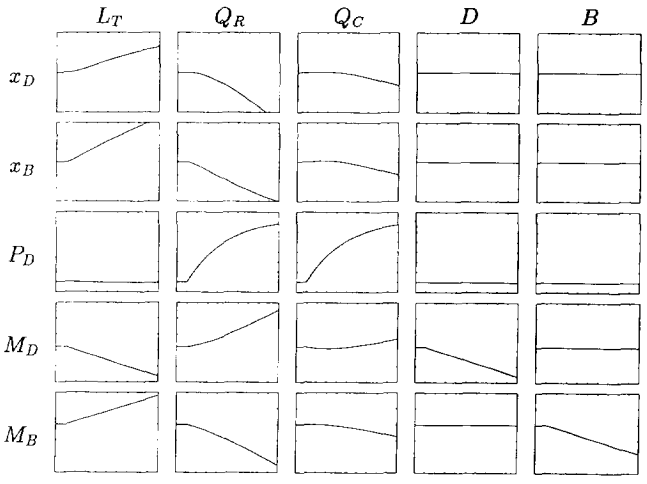

Figure 2 Open loop step responses showing the effect of the five inputs (u) on the five outputs (y). 200 min simulation time. Perturbations and output ranges are displayed in *Table 2*.

The column has 39 trays plus a total condenser and a reboiler, and is modelled using 41 control volumes. It is assumed that each control volume contains a perfectly mixed two-phase system in thermal and vapour–liquid equilibrium. An implicit UV-flash calculation is used to obtain liquid and vapour compositions, temperature and pressure on each tray. This yields a model with three states (differential equations) per control volume (the molar holdup of each component and the internal energy), resulting in a total of 123 states for the column with condenser and reboiler.

Table 1 Column data

Feed (d)	F	= 1.0 (kmol min^{-1})
	$z_F(1)$	= 0.5 (kmol kmol^{-1})
	P_F^{sat}	= 0.11 (MPa)
Controlled outputs (y)	$x_D(1)$	= 0.99 (kmol kmol^{-1})
	$x_B(1)$	= 0.01 (kmol kmol)
	P_D	= 0.1 (MPa)
	M_D	= 32.1 (kmol)
	M_B	= 11.0 (kmol)
Manipulated inputs (u)	L_T	= 2.724 (kmol min^{-1})
	Q_R	= 128.85 (MJ min^{-1})
	Q_C	= −129.02 (ML min^{-1})
	D	= 0.5 (kmol min^{-1})
	B	= 0.5 (kmol min^{-1})
Key hydraulic parameters	$\bar{\tau}_L$	≈ 2.4 (s)
	$\Sigma\tau_L$	≈ 93 (s)
	$K_{2(Top)}$	≈ 0.5
	$K_{2(Bot)}$	≈ 0.8
Thermodynamic data	Relative volatility, α	= 1.5
	$c_{PL1} = c_{PL2}$	= 150 (KJ kmol^{-1} K^{-1})
	$c_{PV1} = c_{PV2}$	= 75 (KJ kmol^{-1} K^{-1})
	$H_{vap,1}$ @ 65.1 °C	= 40 (MJ kmol^{-1})
	$H_{vap,2}$ @ 75.0 °C	= 40 (MJ kmol^{-1})

Table 2 Data used in *Figure 2*

Input	Perturbation at t = 20 min				
L_T	2.724	to	2.729	kmol min^{-1}	(0.18%)
Q_R	128.849	to	129.049	MJ min^{-1}	(0.16%)
Q_C	−129.018	to	−128.818	MJ min^{-1}	(0.16%)
D	0.500	to	0.505	kmol min^{-1}	(1.00%)
B	0.500	to	0.505	kmol min^{-1}	(1.00%)

Output	Range			
x_D	0.987	to	0.993	kmol kmol^{-1}
x_B	0.007	to	0.013	kmol kmol^{-1}
P_D	0.099	to	0.107	MPa
M_D	31.000	to	33.500	kmol
M_B	9.500	to	12.000	kmol

The nonlinear model has been implemented in the equation oriented simulation package SPEEDUP[7]. This package has been used to obtain the steady-state solution and to linearize the system. The dynamic open-loop responses presented in this paper (*Figure 2*) were also obtained by using SPEEDUP, while the closed-loop responses are linear simulations performed in MATLAB.

A summary of the column data is given in *Table 1*. Open-loop time responses are summarized in *Figure 2* and *Table 2*. Note that a perturbation of Q_C yields inverse responses in all outputs except in P_D. The heat duties, Q_R and Q_C, are defined positive if heat is added to the reboiler and condenser, respectively. Also note that we assume that the heating and cooling duties are adjusted directly, that is, there is no self-regulation and Q_R and Q_C are not affected by changes in pressure and temperature in the column. This may be the case, for example, if heat is provided by condensation, and cooling is provided by boiling. This assumption yields a very long time constant for the open-loop pressure response, and it may be estimated to be about $(M_L + 4M_V)/F = 74$ min, where M_L and M_V are the total liquid and vapour molar holdups in the column, condenser and reboiler, and F is the molar feed flow. This formula is derived from an overall heat balance assuming that the temperature change is the same throughout the column. The factor 4 for the vapour holdup is a typical value, and is due to the fact that $c_{PV} > c_{PL}$ and that some energy is needed for evaporation when pressure increases. If we have self-regulation in the condenser, e.g., $Q_C = UA(T_{cool} - T_D)$ with T_{cool} as an independent variable rather than Q_C, we get $F + UA/c_{PL}$ in the denominator instead of F, and the time constant is much smaller, typically about 2 min.

Controllability analysis

In this section simple linear tools (e.g., Wolff *et al.*[8]) are used to assess the controllability properties of the plant, that is, to evaluate any inherent performance limitations. The results from the controllability analysis are also used to specify realistic requirements for control performance and thereby reduce the need for iterative adjustments of the performance requirements, i.e. the 'weights' used to tune the controller.

Conclusions drawn from some of the measures, such as the inputs required for perfect control or the presence of RHP zeros, are valid independently of the control algorithm, while some other measures (CLDG, PRGA) only apply to decentralized control.

The model used in this section was obtained by linearizing the non-linear model using the linearization package CDI within SPEEDUP and then reducing the number of states from 123 to 15, using 'ohkapp' from Robust Toolbox[9]. The open-loop model of the plant has two pure integrators namely the holdups in reboiler and condenser. These pure integrators may cause numerical problems for CDI and for the model reduction routine. To avoid this problem, the levels are stabilized in the non-linear model, before linearization, using very low proportional feedback from the levels to D and B, respectively, thereby placing the eigenvalues at −0.0001 instead of 0.

Scaling

RGA, poles and zeros are independent of scaling, but most other measures depend critically on scaling. Therefore, all results and plots in the following are in terms of scaled variables, i.e., all outputs, setpoints, inputs and disturbances are scaled by 'the maximum acceptable deviation (mad)' from the desired operating condition of each variable, such that the scaled variables stay within ±1 if the acceptable deviation limits are not violated. The values used for scaling are tabulated in *Table 3*. For example, the scaled reflux (input) is $u_1 = \Delta L_T/L_{Tmad}$, where L_{Tmad} is the maximum allowed deviation in reflux. From *Table 3* $L_{Tmad} = 2.7$ kmol min^{-1}, and since this is equal to the nominal flow, we get that $u_1 = -1$ corresponds to zero reflex and $u_1 = +1$ corresponds to a reflux of 5.7 kmol min^{-1}.

Note that the performance requirement for the levels are very lax, as the allowed error in *Table 3* (30.0 and 10.0) is much larger than the allowed setpoint change (0.5 and 0.5). This is reasonable since we have no strict requirements for level control, but rather want to use variations in level to avoid sudden changes in the product flows, D and B.

Relative gain array (RGA)

The RGA[10] was originally introduced as a steady state interaction measure and as a tool for input–output pairing for decentralized control. However, the RGA may be computed frequency-by-frequency and used to assess the interaction at frequencies other than zero, and also to analyse sensitivity to input uncertainty for multivariable control[11]. The frequency dependent RGA for a

Table 3 Maximum acceptable deviation (mad) for used scaling. (Units and order of elements for these vectors are given in *Table 1*.)

Output error	y_{mad}	= [0.01 0.01 0.050 30. 10.]^T
Setpoints	r_{mad}	= [0.01 0.01 0.0250 0.5 0.5]^T
Inputs	u_{mad}	= [2.7 130 130 0.5 0.5]^T
Feed disturbances	d_{mad}	= [0.15 0.1 0.025]^T

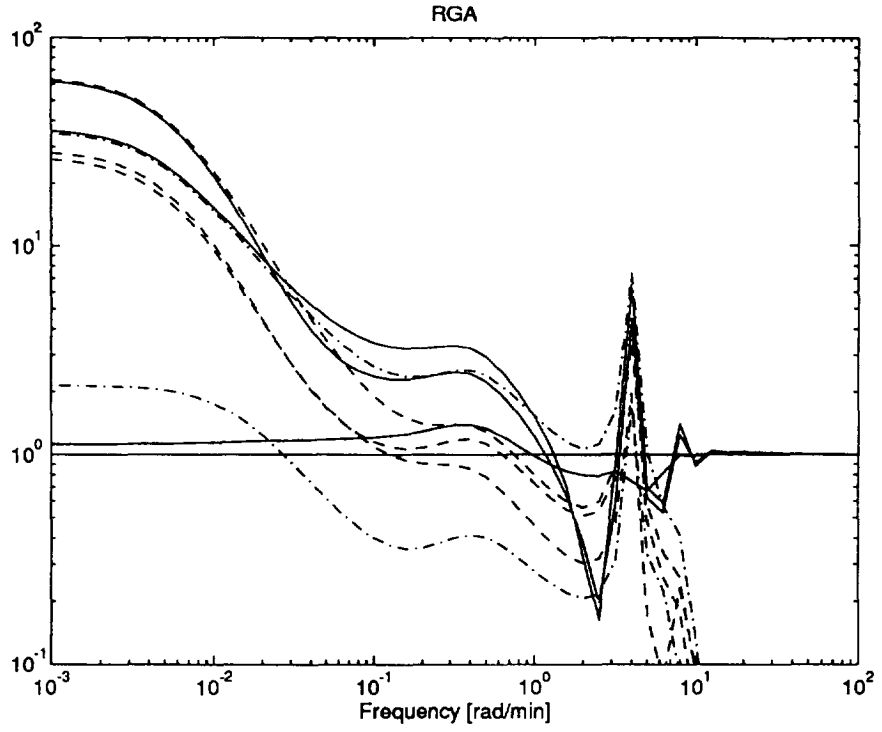

Figure 3 Relative gain array elements as function of frequency (solid lines: diagonal elements)

square system G is defined by $RGA(\omega) = G(j\omega) \times (G^{-1}(j\omega))^T$, where the symbol $\times$ denotes element-by-element multiplication.

The steady state RGA for the linearized 5 × 5 plant is:

	L_T	Q_R	Q_C	D	B
x_D	36.76	−64.65	28.88	0.00	0.00
x_B	−35.72	63.49	−26.76	0.00	0.00
P_D	−0.04	2.16	−1.12	0.00	0.00
M_D	0.00	0.00	0.00	1.00	0.00
M_B	0.00	0.00	0.00	0.00	1.00

(1)

We see that there are strong two-way interactions in the upper left 3 × 3 subsystem, while the condenser level and distillate flow (M_D and D) and the reboiler level and bottoms flow (M_B and B) form two decoupled 1 × 1 subsystems. The physical explanation for the latter is that manipulation of D affects M_D, and B affects M_B, but has almost no influence on the other outputs.

The RGA elements (RGA_{ij}) as function of frequency are shown in *Figure 3* with the diagonal RGA elements ($i = j$) as solid lines. We see that the RGA elements decrease as frequency increases, but there are significant interactions also at frequencies corresponding to the expected closed loop bandwidth ($\Omega \approx 0.1$ rad min^{-1}).

The 3 × 3 interaction for the composition and pressure subsystem could in principle (if there was no uncertainty) be corrected for by a multivariable controller, for example a decoupler. However, the large RGA elements (*Figure 3*) at frequencies around the closed-loop bandwidth signal high sensitivity to diagonal input uncertainty[11] and thereby prevent the use of a decoupler. Thus, we may already at this stage conclude that it is essential to consider input uncertainty when tuning a multivariable controller for this plant.

RHP zeros

The 5 × 5 model has no multivariable right half plane (RHP) zeros. However, there are RHP zeros in several elements of the 5 × 5 model, as shown from the inverse responses in *Figure 2*. Specifically, a change in cooling duty Q_C yields inverse responses for all outputs, except for the pressure. The main reason behind this is that a change in Q_C, with the other manipulated inputs kept constant, yields an inverse response for the vapour flow V_T entering the condenser. Initially, an increase in cooling yields a fast increase in V_T. However, with increased cooling, Q_C, and constant heating, Q_R, the column temperature starts decreasing, and the heat of vaporization increases leading to a steady state decrease in $V_T = Q_C/H^{vap}$. The inverse responses in the outputs are very slow (zero locations: $z_{13} = 0.0367$; $z_{23} = 0.0264$; $z_{43} = 0.0204$; $z_{53} = 0.0580$ min^{-1}), so for single-loop control the cooling duty can only be used to control the pressure. However, this means pairing on a negative RGA-element and results in the complications described in the previous section. Using the results from Hovd and Skogestad[12] we know that the negative RGA (3,3-element) must imply that there is a RHP transmission zero in the remaining subsystem, since there is no RHP zero in the 3,3 SISO-element itself and no 5 × 5 RHP transmission zeros. Indeed, we find that the upper 2 × 2 system (from L_T and Q_R to x_D and x_B) has a RHP transmission zero at 0.0129 min^{-1} (the lower 2 × 2 sys-

tem, from D and B to M_D and M_B, is decoupled and does not influence this value). This RHP transmission zero implies that fast control of both compositions (closed loop bandwidth less than about 75 min) requires that the pressure controller is functioning, if SISO pressure control paired on the 3,3 element is used.

Input saturation

Input saturation imposes a fundamental limitation on the control performance. The inputs required for perfect control are $u = G^{-1}r + G^{-1}G_d d$. Thus, in terms of scaled variables the elements in the matrices G^{-1} and $G^{-1}G_d$ should be less than 1 in the frequency range where control is needed. For our example, with the allowed variations in the inputs as given by u_{mad} in *Table 3*, we find from frequency-dependent plots of the elements of these matrices (not shown) that input saturation is not a serious problem for this plant, not even at relatively high frequencies.

Decentralized control

Controllability analysis

Consider again the steady-state RGA in Equation (1). The conventional 'LV-configuration', which is considered for the decentralized controller in this paper, corresponds to pairing on the diagonal elements.

The first observation from the steady-state RGA is that the 4,4 and 5,5 elements are 1.0 while all other elements in columns 4 and 5 and rows 4 and 5 are zero. Following the conventional pairing rule for decentralized control we should pair on elements close to 1, i.e. use D to control M_D and B to control M_B. Also, since manipulation of D affects M_D, and B affects M_B, but has almost no influence on the other outputs, it follows that composition control is insensitive to the tuning of the level loops. This is one of the main advantages with the LV-configuration. (One possible advantage with other configurations, such as the DV-configuration, is that the closure of the level loops affects the composition control such that the interactions are reduced, for example as expressed in terms of the RGA for the remaining 2 × 2 composition control problem.)

The second observation is that the 3,3 element is negative. From the results of Grosdidier *et al.*,[13] we know that a decentralized control scheme with integral action paired on this negative RGA element leads to:

1. The overall system is unstable, or
2. The pressure loop is unstable, or
3. The remaining system is unstable if the pressure loop fails.

In practice, this means that using Q_C to control P_D and tuning for a stable pressure loop and a stable overall system leads to instability if the pressure loop fails, e.g. if Q_C saturates. Thus, one must be very careful to avoid saturation in the pressure loop if decentralized LV control is used.

Remark. Note that we assume in this paper that the heat duties Q_C and Q_R are independent variables. If self-regulation was included, for example by manipulating T_{cool} or T_{heat}, then the negative RGA-element will most likely disappear.

From the frequency-dependent RGA plot in *Figure 2* we note that the diagonal elements are fairly large (about 3) also in the frequency region important for control, $\omega \approx 0.1$ rad min^{-1}. Thus, we can expect interactions at these frequencies when decentralized control is used.

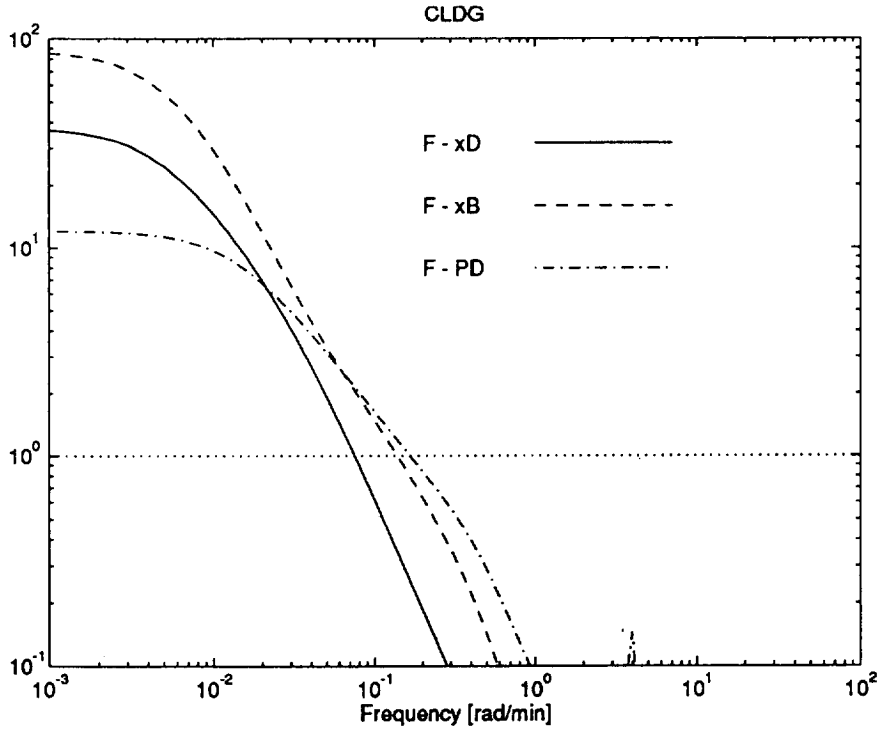

Figure 4 Closed loop disturbance gain for decentralized control

The RGA is useful for selecting pairings. However, to evaluate decentralized performance for setpoint changes the Performance RGA, which is scaling dependent, is the appropriate tool. The PRGA is not shown here, but one main finding is that the worst setpoint change is for top composition, $x_{D,s}$, and in particular that a strong interaction is expected for the pressure.

The closed-loop disturbance gains (CLDG) yield the effect of disturbances under decentralized control. For all outputs the worst disturbance is the feed rate F, and the effect of this disturbance is given in *Figure 4*. The bandwidth requirement for rejecting a 15% disturbance in F is about 14 min for top composition (x_D), 7 min for bottom composition (x_B) and 6 min for top pressure (P_D).

Simulations with LV configuration

One conclusion from the controllability analysis is that it is difficult to obtain very good control performance with decentralized control due to the strong 3 × 3 interaction. This is confirmed by the simulation in *Figure 5* which shows the response to a setpoint change $x_{D,s}$ (at t = 0 min) and to a step increase in the feedrate F (at t = 100 min). Note that these two upsets were identified as the most difficult ones to handle by the controllability

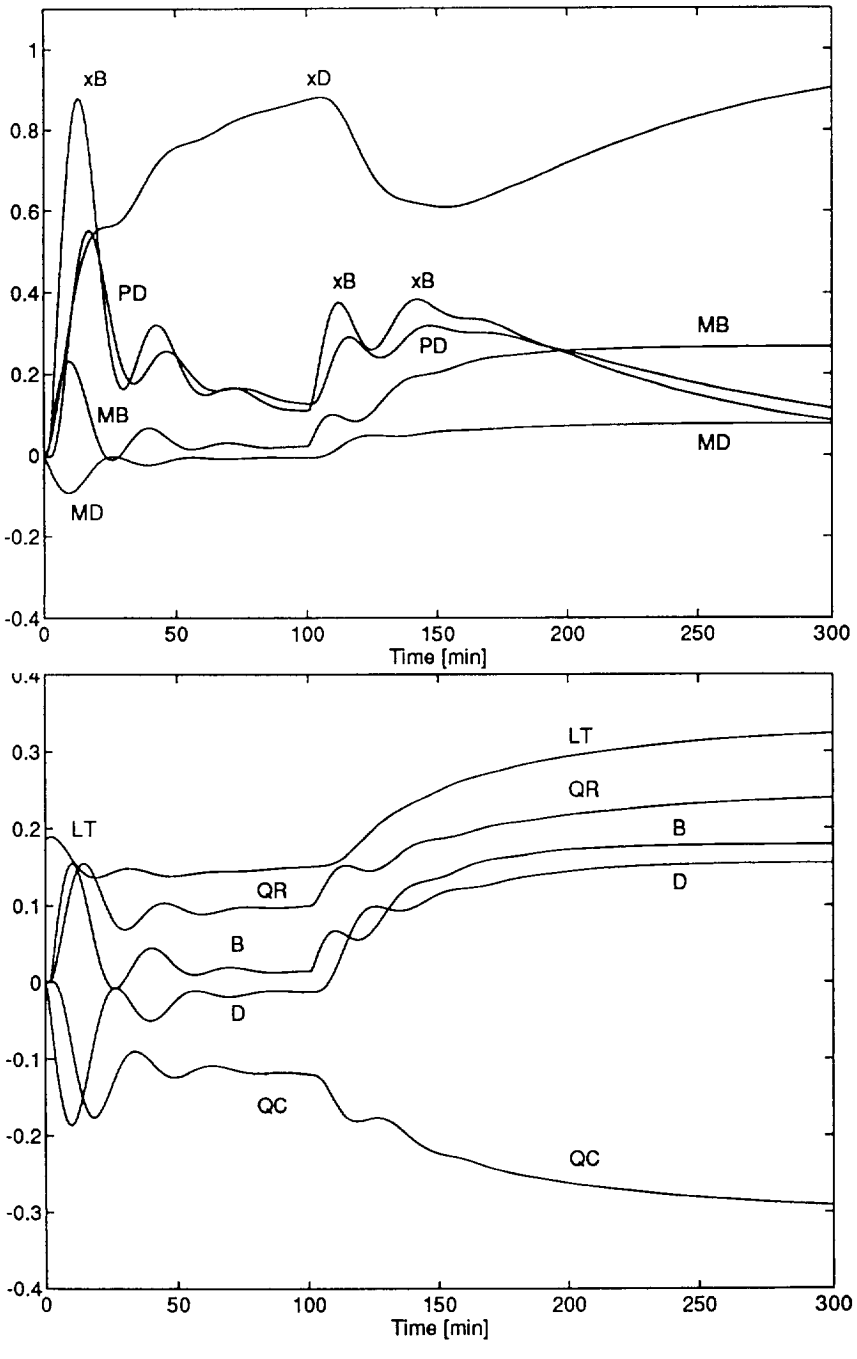

Figure 5 Simulated decentralized control performance for setpoint change in x_D at t = 0 and 15% feed disturbance at t = 100 min. Upper plot: scaled controlled outputs. Lower plot: scaled manipulated inputs

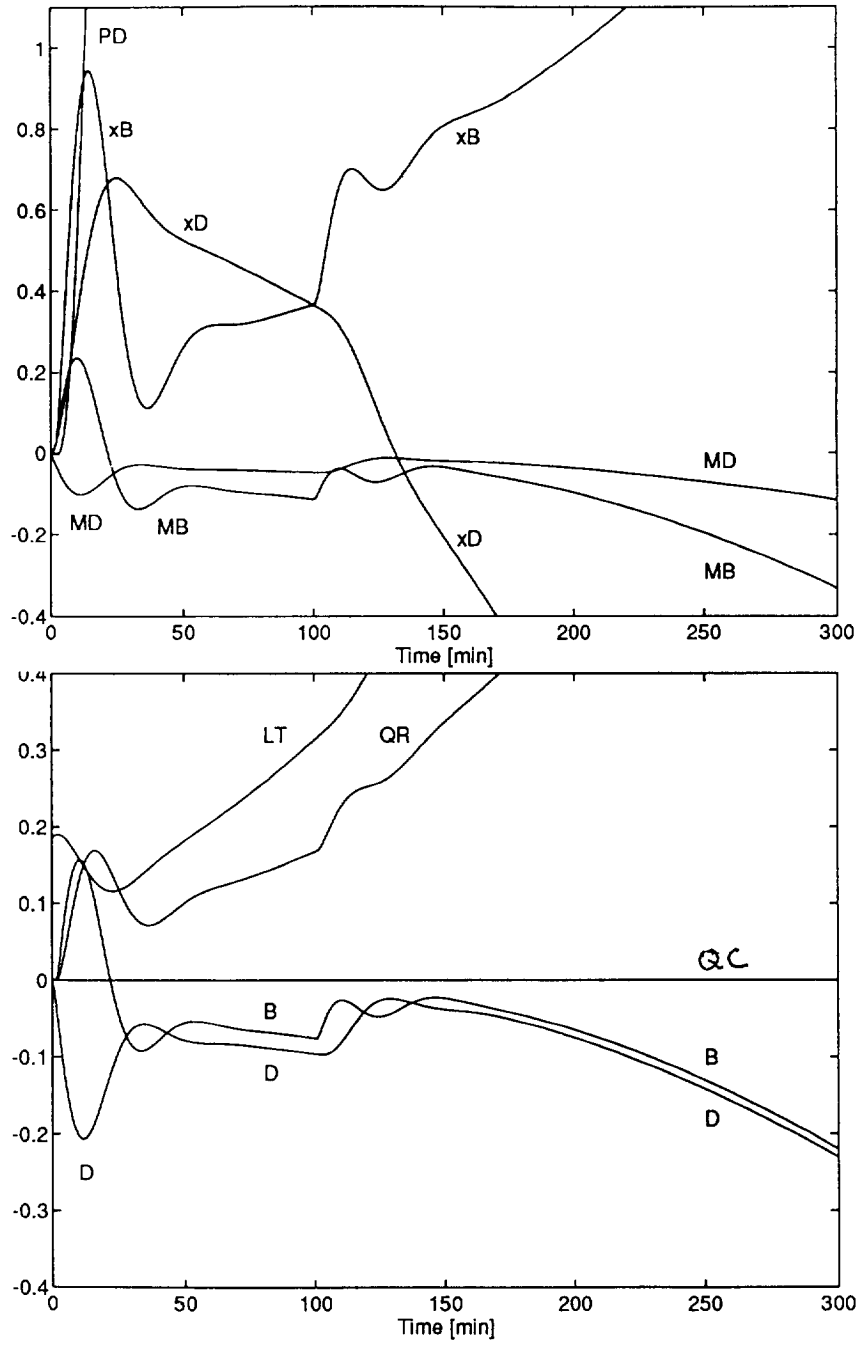

Figure 6 Simulated decentralized control performance with constraint on cooling ($Q_c \geq 0$), for setpoint change in x_D at $t = 0$ and 15% feed disturbance at $t = 100$ min. Upper plot: scaled controlled outputs. Lower plot: scaled manipulated inputs

analysis. In the controllability analysis we also predicted that we would encounter instability if the pressure loop failed due to the negative 3 × 3 element in the steady-state RGA. This is confirmed by the simulation in *Figure 6* where we have introduced the constraint that we cannot allow any more cooling than the nominal value of −128.85 MJ min^{-1} (in terms of scaled deviation variables presented in the figure the constraint is that $Q_C \geq 0$).

The controllers used in the simulations were tuned to yield a closed loop time constant of 3 min for the pressure loop, about 15 min for top composition x_D and 8 min for the bottom composition x_B (individually, i.e. without considering interactions). The level loops, which have essentially no effect on the rest of the system, were very loosely tuned to closed loop time constants of 30 min.

$\mathcal{H}_\infty/\mu$ control

Weight selection

In this section we study the unconstrained control problem using the $\mathcal{H}_\infty/\mu$ framework. The purpose is to study possible improvements in performance with multivariable control. The $\mathcal{H}_\infty$-norm is used because it is rather straightforward to specify the desired responses in terms

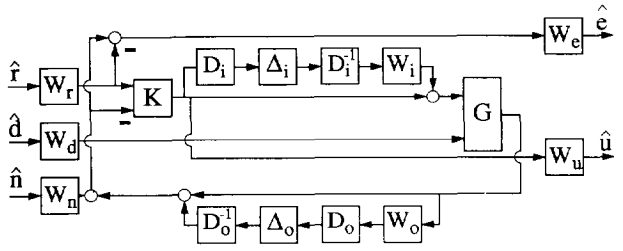

Figure 7 Block diagram for robust $\mathcal{H}_\infty$-problem

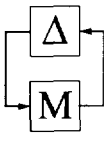

Figure 8 $M - \Delta$ structure for μ-analysis

of 'classical' measures such as closed-loop time constants, allowable steady state offset and acceptable overshoot. Furthermore, one significant advantage with the $\mathcal{H}_\infty$-norm is that it allows worst-case model uncertainty to be included explicitly (using the structured singular value, denoted SSV or μ).

The block diagram in *Figure 7* defines the problem studied in this section. K is the controller to be designed. It may be a two-degree-of-freedom (TDF) controller with separated inputs r (setpoint) and y_m (measured outputs) as in the figure, or with a one-degree-of-freedom controller (ODF) with input $r - y_m$.

G is the normalized (scaled) plant model with eight inputs (five manipulated inputs u and three unmeasured disturbances d) and five outputs y. The scalings used for the normalization of G are given in *Table 3*. W_r, W_d and W_n are weight matrices for setpoints r, disturbances d and measurement noise n, respectively. W_e and W_u are weights on deviation from desired setpoint, e, and manipulated inputs, u, respectively. The weighting matrices are diagonal with elements $[W_r] = r_{mad}/y_{mad}$, $[W_d] = 1$, $[W_n] = 0.01$, $[W_u] = 1$ and

$$[W_e](s) = \frac{1}{M_s}\frac{\tau_{cl}s + M_s}{\tau_{cl}s + A};\ M_s = 2,\ A = 0.0001 \qquad (2)$$

with τ_{cl} = [30 30 30 60 60] min. For the compositions, for which the setpoints r and controlled outputs y have identical scalings, M_S is the maximum allowed peak of the sensitivity function and τ_{cl} is the required closed-loop response time for that output. Note that A is very small so that integral action is in practice required for all outputs.

Model uncertainty is represented by $W_i D_i^{-1}\Delta_i D_i = W_i\Delta_i$ which models input uncertainty, and $D_o^{-1}\Delta_o D_o W_o = \Delta_o W_o$ which models output uncertainty. Δ_i (and Δ_o) is any diagonal matrix with $\mathcal{H}_\infty$-norm less than one, and the Ds are scalings for the μ-problem as discussed below. $W_i = 0.1 \cdot I_{5\times5}$ and $W_o = \{\theta s/(0.5\theta s+1)\} \cdot I_{5\times5}$, corresponding to 10% relative gain uncertainty in each input, and a delay of up to approximately $\theta = 1$ min in each measurement.

Table 4 Controller element-by-element modulus at $\omega = 0.01$ rad min^{-1}

	e_{xD}	e_{xB}	e_{PD}	e_{MD}	e_{MB}
L_T	1.4289	0.3660	0.2290	1.1815	0.7863
Q_R	0.1913	0.9435	0.4865	0.3867	0.4439
Q_C	0.3328	0.7201	0.7358	0.4851	0.0370
D	0.0663	0.0339	0.0193	1.3192	0.1242
B	0.0875	0.0986	0.0376	0.3217	0.7884

We arrived at this problem formulation and these weights through several steps, starting with a pure $\mathcal{H}_\infty$-problem with only setpoints and no uncertainty and ending up with the overall μ-problem as defined by *Figure 7*. In the following we shall go through some of these steps because it yields some insight.

Setpoint tracking with no uncertainty

This corresponds to the case with $\hat{d} = 0$, $\Delta_i = 0$, $\Delta_o = 0$ and yields a pure $\mathcal{H}_\infty$-problem for which synthesis software is readily available[9,14]. The optimal controller yields a closed-loop $\mathcal{H}_\infty$-norm equal to 0.83. Since this is less than 1 the performance requirement for the worst case direction is achieved with some margin. The $\mathcal{H}_\infty$-controller uses rather high gains at high frequencies; the 'roll-off' frequency is about 10 rad min^{-1}. This is typical for all the cases we studied and it may be avoided by using a slightly sub-optimal controller with higher $\mathcal{H}_\infty$-norm. This sub-optimal controller yields a blend of $\mathcal{H}_\infty$ and $\mathcal{H}_2$ optimality (which is desirable since our ultimate objective is to use model predictive control which uses the $\mathcal{H}_2$-norm) with 'roll-off' at a lower frequency than the optimal $\mathcal{H}_\infty$-controller, resulting in better robustness with respect to high frequency uncertainty. For this case a sub-optimal controller with $\mathcal{H}_\infty$-norm equal to 1.0 (rather than 0.83) gave approximately the same low-frequency behaviour as the optimal controller, but a 'roll-off' frequency of about 0.2 rad min^{-1}.

The obtained suboptimal controller is a 'full' 5 × 5 controller; however, a more careful analysis of the controller reveals the following two interesting properties.

1) The controller may be decomposed into one 3 × 3 controller for composition and pressure control and two single-loop controllers for the levels, corresponding to a multivariable LV-configuration.
2) The 3 × 3 pressure and composition controller is essentially a decoupler. This may be seen by evaluating the condition number of GK.

These two statements are not true when disturbances and/or uncertainty is considered, as discussed below.

Remarks. For setpoint tracking of this system without uncertainty there is (1) no advantage in using the information from M_D (M_B) to compute manipulated inputs other than D (B); (2) no advantage in computing D (B) based on information from measurements other than M_D (M_B); (3) no advantage with a TDF controller, since there are no uncertainties and no disturbances.

Including model uncertainty

Robust performance analysis of the system in *Figure 7* with model uncertainty is performed by connecting the scaled outputs $[\hat{e}\hat{u}]^T$ to the scaled inputs $[\hat{r}\ \hat{d}\ \hat{n}]^T$ through a 'performance perturbation' Δ_P and then rearranging the system into the $M\Delta$-structure showing in *Figure 8* where $\Delta = \text{diag}\{\Delta_i,\Delta_o,\Delta_P\}$. To analyse such a system we must use the structured singular value, μ instead of the $\mathcal{H}_\infty$-norm. In this paper we use as a tight approximation for μ the scaled $\mathcal{H}_\infty$-norm, $\min_D \|DMD^{-1}\|_\infty$. The structure of the D-scales depend on the model uncertainty. In our case with diagonal uncertainty at the input and the output we get $D = \text{diag}\{D_i,D_o,I_{5\times5}\}$ where D_i and D_o are diagonal matrices each with five entries which are 'adjusted' to minimize the scaled $\mathcal{H}_\infty$-norm above. The μ-optimal controller is then obtained by DK-iteration[15]:

1. K-step. Fix D and obtain K by minimizing the $\mathcal{H}_\infty$-norm $(\min_K \|DM(K)D^{-1}\|_\infty$.
2. D-step. Obtain D-scales by computing μ using the upper bound, $\min_D \|DMD^{-1}\|_\infty$.

These D-scales are frequency dependent and are fitted to low order transfer functions. One iterates between these two steps until convergence. Note that convergence to the μ-optimal controller is not guaranteed with this procedure, although it usually works well if the problem is reasonably scaled to begin with. Usually only a few iterations are performed such that a sub-optimal μ-controller is obtained.

Setpoint tracking with input uncertainty

To consider the effect of model uncertainty we added input uncertainty (but no disturbances or output uncertainty) and obtained an ODF controller by DK-iteration. Actually we found that the controller obtained by using $D_i = I_{5\times5}$ was almost as good as any other controller. It yields $\mu_{RP} = 0.938$. This value could possibly be reduced a few percent by a more sophisticated higher order D-scale, but after a few DK-iterations with only slightly reduced μ_{RP} we decided to use $D_i = I_{5\times5}$. This choice leads to a low order controller and it also makes it easy to apply the $\mathcal{H}_\infty/\mu$ weights in the MPC design (see next section).

In *Table 4* the gains of the ODF controller at frequency $\omega = 0.01$ rad min^{-1} are given. The main difference between this controller and the controller designed for no uncertainty is that this controller does not invert the plant. Also note that the diagonal elements are the largest elements in each row/column. A second difference is that the level measurements M_D and M_B are not only used to compute D and B but have a major impact also on the other manipulated variables. However, note that D and B are almost only affected by M_D and M_B. We found that this $\mathcal{H}_\infty$-controller can be reasonably well approximated by a decentralized L/D V/B configuration (compare with Equation (11) in Skogestad and Morari[16]). In this scheme D is computed from M_D, B is computed from M_B, but L_T is computed from both x_D and M_D and V is computed from both x_B and M_B. These results are consistent with earlier findings which found that this configuration has much lower RGA-values and is preferable when there is input uncertainty.

Remarks. (1) Here we do not consider any disturbances, and the reason for utilizing the level measurements when computing L_T, Q_R and Q_C must be that the effect of the input uncertainty shows up in these measurements. (2) The required bandwidth for the pressure response is not very high; however, the controller tuned for input uncertainty 'chooses' to use a high pressure bandwidth to reduce the effect of the uncertainty. (3) A two-degrees-of-freedom controller improves the performance in this case. It yields $\mu_{RP} = 0.94$ using $D_i = I_{5\times5}$. Again this is explained by the fact that the uncertainty acts as a disturbance.

Including disturbances and output uncertainty

Including disturbances and output uncertainty to the problem yields the system shown in *Figure 7*. This system will after a few DK-iterations yield a controller of rather high order, due to the D-scales. To avoid this high order controller, we use a problem formulation without output uncertainty when synthesizing the controller, and then check the performance using μ-analysis on the full problem.

It turns out that the neglected measurement delays (high frequency output uncertainty) can be dealt with by using a sufficienty sub-optimal $\mathcal{H}_\infty$-controller. The finding from the previous section, that $D_i = I_{5\times5}$ is a good D-scale simplifies the design even further to a pure $\mathcal{H}_\infty$-problem.

The controller used for the simulations shown in *Figure 9* was obtained by $\mathcal{H}_\infty$-synthesis using a problem with setpoint changes, disturbances, noise and input uncertainty, but without output uncertainty. To obtain robustness w.r.t. the neglected measurement delays (high frequency output uncertainty), we synthesized a sub-optimal $\mathcal{H}_\infty$-controller with $\mathcal{H}_\infty$-norm 1.35. Then we computed μ for the full problem. μ_{RP} with output uncertainty is 1.21 and μ_{RS} is 0.99, i.e. the performance is not quite as good as required by the weights, but stability is guaranteed for the worst case plant.

The response of this controller is shown by the dashed lines in *Figure 9*. As can be seen, it performs much better than the decentralized controller shown in *Figure 5*.

Final remarks

Some final remarks seem in order. Most of these are in accordance with previous findings.

1) With the scalings used for the plant, the optimal input uncertainty D-scales are close to 1 for all cases. The optimal D-scales for the output uncertainty are about 5.

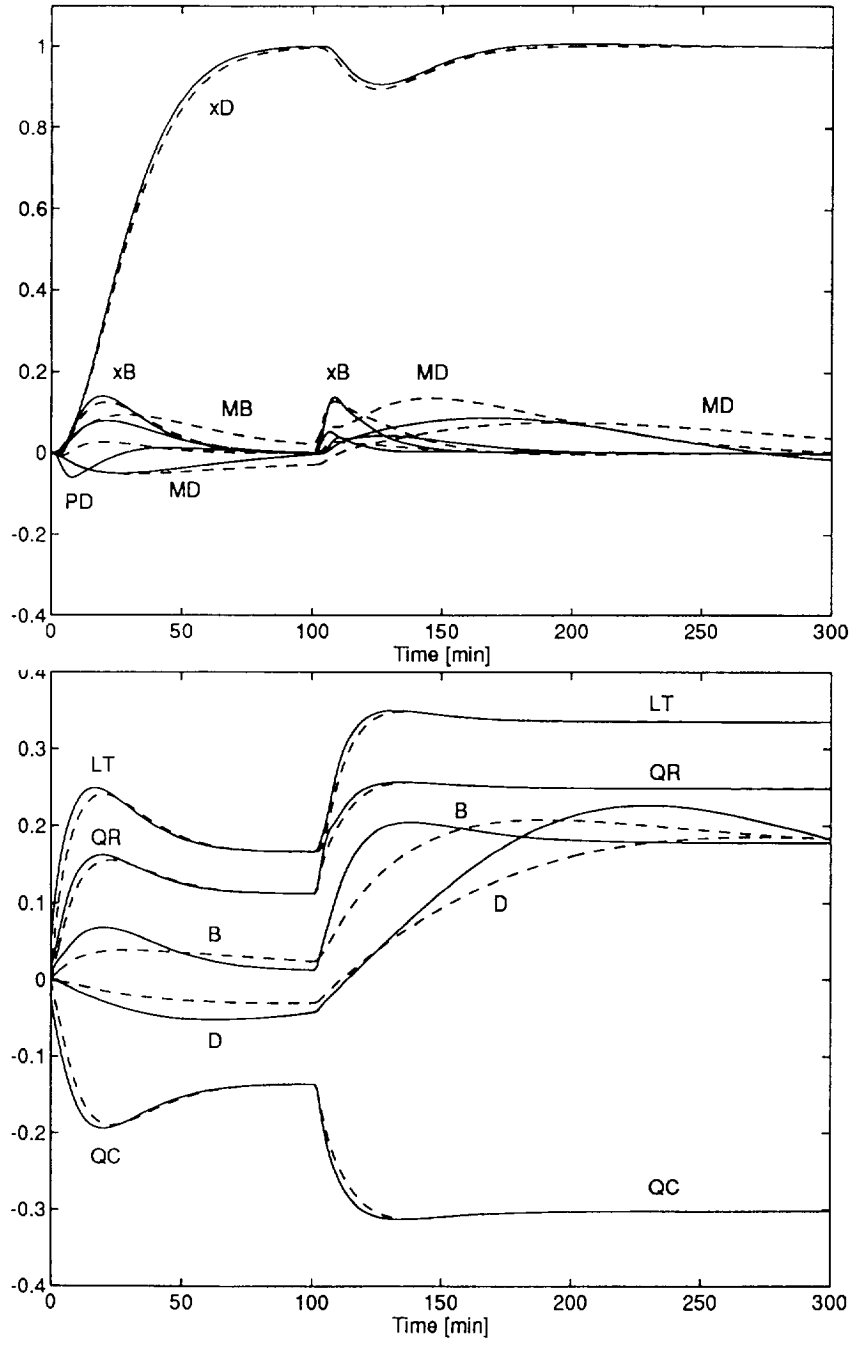

Figure 9 Simulated unconstrained control performance for setpoint change in x_D at $t = 0$ and 15% feed disturbance at $t = 100$ min. Solid lines: MPC. Dashed lines: μ-controller. Upper plot: scaled controlled outputs. Lower plot: scaled manipulated inputs

2) The weights were chosen to yield $\mu \approx 1 \pm 0.2$ for all problems. The reason is that interpretation of μ is difficult if it is too different from 1.
3) A controller designed for setpoint changes only does not perform well if disturbances are considered.
4) A controller designed without considering input uncertainty performs poorly with input uncertainty.
5) A controller designed without considering output uncertainty performs well if the controller is slightly $\mathcal{H}_\infty$ sub-optimal.

Model predictive 5 × 5 control

In this section we use a model predictive control algorithm which involves constrained on-line optimization over a finite receding horizon to explicitly address input constraints. There are several different variants of these schemes, but they differ mainly in the way that future outputs are predicted. The commonly used QDMC algorithm[17] makes the crude assumption that all disturbances act as steps on the outputs, but as shown by Lundström *et al.*[18] this may lead to poor results when

both compositions are controlled. Therefore, we use a state observer based MPC algorithm with a constant Kalman filter gain*. The tuning parameters for this MPC controller are: H_p the output prediction horizon, H_c the control horizon, Λ_y output weight, Λ_u input weight and K_f the Kalman filter gain. The filter gain is a function of the disturbance model and the disturbance and noise covariance matrices.

Recently Lee and Yu[19] presented tuning rules for obtaining robust MPC performance. For the case of diagonal input uncertainty they penalize the input moves using Λ_u in order to obtain robustness. Applying this method to the distillation problem from Skogestad *et al.*[20] gave $\mu_{RP} = 2.23$, whereas the optimal value is known to be less than 0.978[21]. This is not satisfactory, and therefore, in this paper we do not use the input weight Λ_u, but the observer parameters to obtain robustness with respect to input uncertainty.

Our main objective is to use the weights obtained from the rigorous robustness analysis in the previous section as a starting point for weight selection for the MPC controller. There are several difficulties here. First, the MPC scheme uses the $\mathcal{H}_2$-norm rather than the $\mathcal{H}_\infty$-norm. Second, the MPC controller is a finite horizon controller which contains additional tuning parameters. Third, uncertainty can not be included explicitly.

In spite of these difficulties, we were able to tune the MPC controller to mimic the μ-controller very closely. One reason for this success is probably that the $\mathcal{H}_\infty/\mu$-controller is sub-optimal and therefore '$\mathcal{H}_2$-ish' and easier to mimic with MPC. The final tuning of the response time was done by adjusting a single parameter α in the output weight to minimize μ in the robustness problem defined in the previous section. The input uncertainty was in the MPC design represented by opening the loop through Δ_i (*Figure 7*), which results in a weight (D_i) penalizing the use of u and a disturbance weight ($W_i D_i^{-1}$) acting on the plant inputs. Output uncertainty was not included since the robustness analysis found that this uncertainty was not crucial. The tuning parameters are summarized next.

Optimization part of MPC controller. Sampling time: 1 min, horizons $H_p = 60$ and $H_c = 3$.

$$\Lambda_y = \alpha W_e; \quad \Lambda_u = |W_u| + |D_i| \tag{3}$$

(where W_e and W_u are the $\mathcal{H}_\infty$-weights and D_i and D-scale representing the input uncertainty).

Kalman filter part of MPC controller. Augmented disturbance model to include model uncertainty

$$G_d = C(sI - A)^{-1}B = G \operatorname{diag}\{W_i D_i^{-1}, W_d\} \tag{4}$$

This leads to the Kalman filter gain $K_f = P_f C^T V^{-1}$ where P_f is obtained by solving the Riccati equation $P_f A^T + A P_f - P_f C^T V^{-1} C P_f + BWB^T = 0$ where the covariance matrices for disturbance is $W = I_8$ and for noise is $V = W_n^2$.

The optimal value of α (Equation 3), for the same problem specification as in the previous section, was found iteratively. For a chosen value of α we obtained the frequency response of the discrete controller, added zero order hold elements at the outputs of the controller and computed μ. After some iterations, a value $\mu = 1.15$ was obtained for $\alpha = 0.03$. The linear robust performance was thus in fact somewhat better than the sub-optimal $\mathcal{H}_\infty$-controller obtained earlier.

The solid lines in *Figure 9* show the simulated performance of the MPC controller when no constraints are active, that is, when it behaves like a linear controller. The response is seen to be very similar to the μ-optimal controller found previously (dashed lines). The main difference is the speed of response of the levels and the use of inputs D and B.

Figure 10 shows the MPC responses when Q_C is constrained to be at its nominal value. As we see, the MPC controller preserves stability, and manages to keep the levels and the pressure close to their desired values. However, the composition control is relatively poor since the compositions can not be maintained at their setpoints when one degree of freedom is lost.

Some final remarks

1. In the simulations we used a 1 min delay in each measurement and used −10% input gain error in all inputs expcept Q_R which has +10% uncertainty†.
2. The unconstrained simulation shows that the controller performs well both for setpoint tracking and disturbance rejection. No excessive input usage is required. The performance for the outputs in *Figure 9* is significantly better than for the decentralized scheme shown in *Figure 5*.
3. In the constrained case the use of a MPC scheme avoids the need for complicated logics including overrides and retuning. If the decentralized control scheme from the Section on controllability analysis is used, then the system goes unstable when Q_C is fixed. The multivariable μ-controller does not go unstable, but performs very poorly, and simulations show that it goes unstable when Q_R is fixed.
4. In the simulations there was given no forewarning about the desired setpoint change at $t = 0$. Most controllers are causal and would not be able to make use of this information, but in many MPC implementations such information may be used. For example, if at $t = -100$ min the MPC optimizer was told that a setpoint change is desired at $t = 0$, then it would immediately start changing the inputs to make the transition as optimal as possible.

*The MPC controller we use here is from the program 'scmpc' in the MPC-toolbox for MATLAB[3].

†This input uncertainty was found to be the worst of all ± 10% combinations.

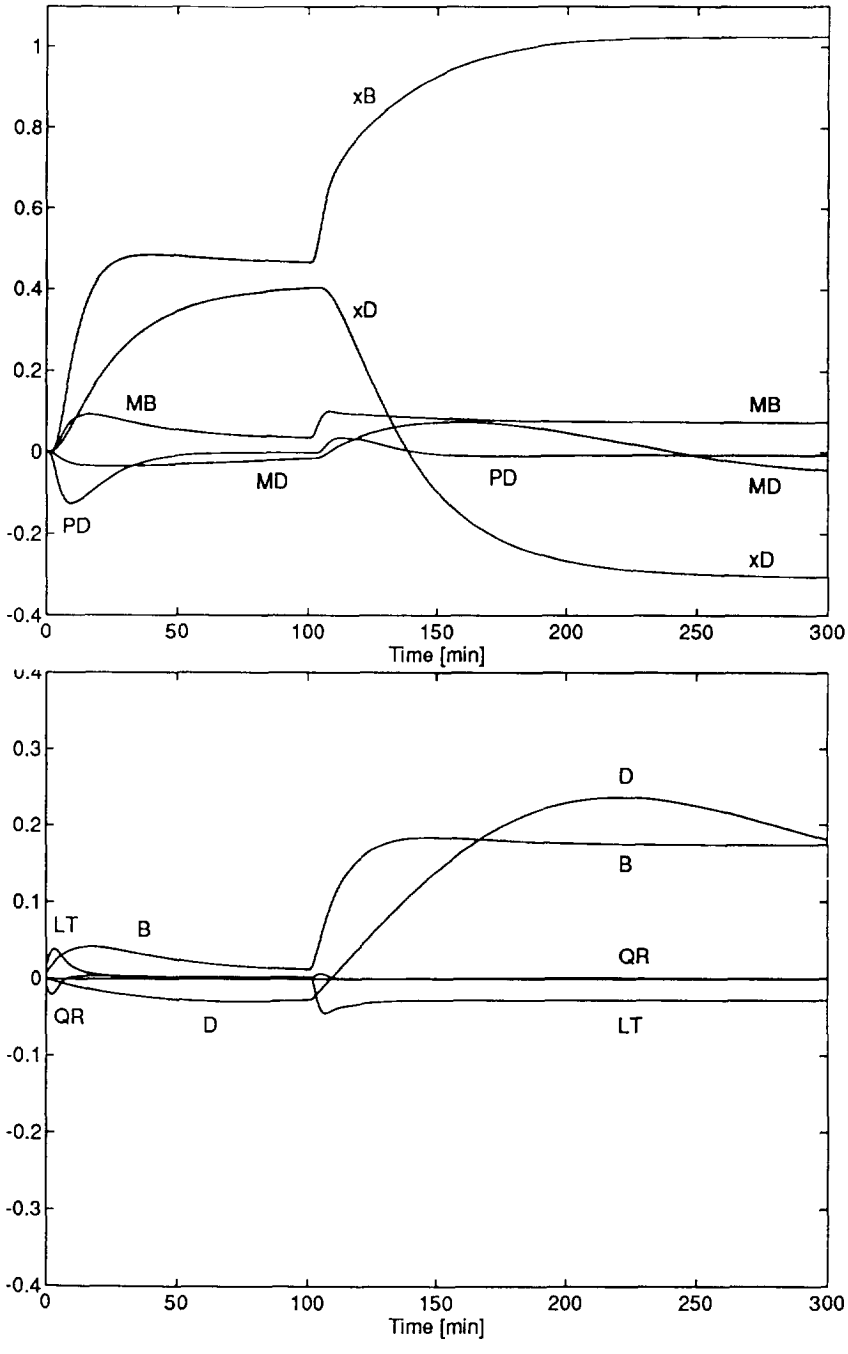

Figure 10 Simulated MPC performance with constraint $Q_C > 0$, for setpoint change in x_D at $t = 0$ and 15% feed disturbance at $t = 100$ min. Upper plot: scaled controlled outputs. Lower plot: scaled manipulated inputs

Discussion

It is often desirable to use a compensator-based controller which retains some of the simplicity of a decentralized controller, that is, $K = C_1 K_{diag}(s) C_2$ where C_1 and C_2 are fixed matrices (or at least contain very simple dynamics) which take care of the interactions whereas K_{diag} consists of simple single-loop controllers to take care of the dynamic effects. One insight from analysing the optimal multivariable controllers is that a precompensator C_2 (mixing of measurements, that is use level measurement also for composition control) is useful, while a postcompensator C_1 (mixing of inputs) is less useful due to the presence of input uncertainty. A pure precompensator scheme is sometimes implemented as a regular decentralized control scheme, but with a 'feed-forward' action from the disturbances, where disturbances are estimated from level and pressure measurements. Another insight is that a multivariable prefilter (two degrees of freedom controller) may reduce the interactions for setpoint changes. Although such schemes may improve the multivariable properties of the controller, they will still need special logics to handle constraints.

The reboiler and condenser holdups of a distillation column (and to some extent also the pressure) do not

have to be tightly controlled, but may be considered 'slack' output specifications. The slackness of these specifications yields a system which may be viewed as a temporarily non-square system with access of inputs. That is, as long as the levels M_D and M_B are within their upper and lower limits we may use all five inputs L_T, Q_R, Q_C, D and B to control three outputs x_D, x_B, and P_D. At first one may believe that the 'freed' inputs may be used to improve control performance. However, in the case of a distillation column, the 'freed' variables D and B are not effective for controlling x_D, x_B or P_D, so the slack level requirements cannot be used to improve the composition or pressure control; however, the slack specifications are often used to eliminate fast variations of the inputs D and B.

Conclusions

The results in this paper indicate that the main advantages with 5 × 5 distillation control are the improved disturbance detection by indirect use of the level and pressure measurements, and the explicit input constraint handling. One difficulty is the tuning of the controller, but in our example we were able to tune the MPC scheme quite easily to get acceptable robustness. The following procedure was used: (1) Define a robust $\mathcal{H}_\infty$-problem with an optimal μ-value close to 1. (2) Use the weights and scaling found for this problem to derive MPC tuning parameters. The critical uncertainty, in this case at the inputs, is represented as fictitious disturbances. (3) One adjustable parameter in the MPC controller is used to minimize μ. (4) Time simulations are used to check the results and possibly adjust some weights. The resulting controller is not 'optimal' in any mathematical sense, but was found to perform very well.

In terms of the distillation model we have assumed that the heat duties Q_D and Q_B are independent variables for control. This yields a somewhat unusual behaviour in terms of the open-loop pressure. It would be interesting to study the effect of introducing some mechanism of self-regulation for the pressure by having the heat duties depend on the column temperatures.

References

1 Skogestad, S. 'Modelling and Control of Distillation Columns as a 5 × 5 System', DECHEMA Monographs, 1989, **116**, (ed. R. Eckermann) 403 (From 20th Europ. Symp. on Computer Applications in the Chemical Industry (CACHI 89), Erlangen, Germany, April 1989)

2 Doyle, J.C. *IEE Proc.* 1982, **129**, Part D, 242

3 Morari, M. and Ricker, N.L. 'MPC toolbox for MATLAB,' Californian Institute of Technology, 1991

4 Skogestad, S. and Morari, M. *Ind. Eng. Chem. Res.* 1988, **27**(10), 1848

5 Bennett, D.L., Agrawal, R. and Cook, P.J. *AIChE J.* 1983, **29**(3), 434

6 Rademaker, O., Rijnsdorp, J.E. and Maarleveld, A. 'Dynamics and Control of Continuous Distillation Units', Elsevier, Amsterdam, 1975

7 Pantelides, C.C. *Comput. Chem. Eng.* 1988, **12**(7), 745

8 Wolff, E.A., Skogestad, S., Hovd. M and Mathisen, K.W. 'A Procedure for Controllability Analysis' in 'Preprints IFAC Workshop on Interactions between Process Design and Process Control', London, September 1992, (Ed. J. Perkins) Pergamon Press, Oxford, 1992, 123

9 Chiang, R.Y. and Safonov, M.G. 'Robust-Control Toolbox for MATLAB. User's Guide', The Math Works Inc., Natick, MA, 1992

10 Bristol, E.H. *IEEE Trans. Autom. Control* 1966, **AC-11**, 133

11 Skogestad, S. and Morari, M. *Ind. Eng. Chem. Res.* 1987, **26**(11), 2323 (Also see correction to Eq. 13 in 1988, **27**(5), 898)

12 Hovd, M. and Skogestad, S. *Automatica* 1992, **28**, 989

13 Grosdidier, P., Morari, M. and Holt, B.R. *Ind. Eng. Chem. Fundam.* 1985, **24**, 221

14 Balas, G.J., Doyle, J.C., Glover, K., Packard, A.K. and Smith R. 'The μ-Analysis and Synthesis Toolbox', The MathWorks Inc., Natick, MA, 1991

15 Doyle, J.C. in 'Proc. IEEE Conf. Decision Contr.' San Antonio, TX, 1983

16 Skogestad, S. and Morari, M. *AIChE J.* 1987, **33**, 1620

17 Garcia, C.E. and Morshedi, A.M. *Chem. Eng. Commun.* 1986, **46**, 73

18 Lundström, P., Lee, J.H., Morari, M. and Skogestad, S. in 'Proc. European Control Conference', Grenoble, France, 1991, 1839

19 Lee, J.H. and Y, Z.H. *Comp. Chem. Eng.* 1994, **18**, 15

20 Skogestad, S., Morari, M. and Doyle, J.C. *IEEE Trans. Autom. Control* 1981, **33**(12), 1092 (Also see correction to μ-optimal controller in **34**(6), 672)

21 Lundström, P., Skogestad, S. and Wang, Z.-Q. *Trans. Inst. MC* 1991, **13**(5), 241